Platinum complexes of heteroannularly bridged heterobidentate ferrocenyl diphosphine ligands: their molecular structure and their use in catalytic carbonylation reactions

Thomas Sturm [a], Walter Weissensteiner [a,*], Kurt Mereiter [b], Tamás Kégl [c],
György Jeges [d], György Petőlz [e], László Kollár [e,f,1]

[a] *Institute of Organic Chemistry, University of Vienna, Währinger Straße 38, A-1090 Vienna, Austria*
[b] *Institute of Mineralogy, Crystallography and Structural Chemistry, Technical University of Vienna, Getreidemarkt 9, A-1040 Vienna, Austria*
[c] *Research Group for Petrochemistry of the Hungarian Academy of Sciences, PO Box 158, H-8201 Veszprém, Hungary*
[d] *Department of Chemistry, University of Veszprém, PO Box 158, H-8201 Veszprém, Hungary*
[e] *Department of Inorganic Chemistry, Janus Panonius University, PO Box 266, H-7624 Pécs, Hungary*
[f] *Research Group for Chemical Sensors of the Hungarian Academy of Sciences, PO Box 266, H-7624 Pécs, Hungary*

Abstract

Platinum complexes $PtCl_2(L)$ and $PtCl(SnCl_3)(L)$ of the ferrocenyl diphosphine ligands (L) (*R,R*)-1-diphenylphosphino-2,1′-[(1-diphenylphosphino)-1,3-propanediyl]-ferrocene (**1**), (*R,R*)-1-diphenylphosphino-2,1′-[(1-dicyclohexylphosphino)-1,3-propanediyl]-ferrocene (**2**), (*R,R*)-1-bis(4-fluorophenyl)phosphino-2,1′-[(1-diphenylphosphino)-1,3-propanediyl]-ferrocene (**3**), have been synthesised. Complexes $PtCl_2(1)$ and $PtCl_2(2)$ have been structurally characterised by X-ray diffraction. Both the 'preformed' and the in situ catalysts have been used in hydroformylations of styrene. At low temperature (below 70°C) and with use of the platinum catalysts the prevailing formation of (*R*)-2-phenyl-propanal was observed, while at higher temperatures the formation of the (*S*)-enantiomer was favoured. The palladium catalysts proved to be rather inactive in the hydromethoxycarbonylation of styrene. In the presence of ligand **2** the predominant formation of the linear regioisomer was observed. © 2000 Elsevier Science S.A. All rights reserved.

Keywords: Carbonylation; Hydroformylation; Platinum; Palladium; Ferrocene; Phosphine; Nuclear magnetic resonance

1. Introduction

The importance of carbonylation reactions has initiated many studies describing mainly the range of applicability as well as mechanistic considerations [1,2]. In particular, a large number of simple and functionalised olefins have been investigated aiming primarily towards compounds of practical interest [3]. Large efforts have been made to apply carbonylations and especially hydroformylations to the synthesis of chiral building blocks and biologically important derivatives [4–6].

Hundreds of ligands with different steric and electronic properties, shapes and functionalities have already been tested in various homogeneous catalytic reactions [7], including carbonylation reactions [8,9]. In addition to C_2 symmetrical chiral diphosphines [10–16] also asymmetric diphosphines with phosphino groups in different chemical environments were found to be efficient ligands in enantioselective hydroformylation [17].

Complexes of ferrocene-based chiral diphosphines have also been intensively tested and found to be active catalysts in a variety of enantioselective reactions including hydrogenation, hydrosilylation, cross-coupling reactions, aldol condensation and others [18]. Surprisingly, the exploitation of ferrocene-based ligands in enantioselective carbonylation is almost unprecedented [19,20].

* Corresponding author. Tel.: + 43-1-4277-52111; fax: + 43-1-4277-9521.

E-mail address: walter.weissensteiner@univie.ac.at (W. Weissensteiner)

[1] Also corresponding author.

In this paper we describe the synthesis and characterisation of platinum complexes modified with racemic and enantiopure heteroannularly bridged ferrocenyl diphosphine ligands and discuss their application in platinum-catalysed hydroformylation. We also report on palladium-catalysed hydroalkoxycarbonylation reactions.

2. Results and discussion

2.1. Synthesis of ferrocenyl ligand 3

Like **1** and **2** [21,22], enantiopure **3** has been synthesised in two steps from enantiopure (R)-1,1′-[(1-dimethylamino)propanediyl]-ferrocene, **4** (Scheme 1). Lithiation of **4** with n-BuLi and quenching with chlorobis(para-fluorophenyl)-phosphine led to the aminophosphine **5** which on further reaction with diphenylphosphine in acetic acid gave the diphosphine ligand **3**.

2.2. Synthesis and NMR characterisation of the platinum complexes of ferrocenyl ligands 1, 2 and 3

The enatiomerically pure ligands **1**, **2** and **3** were reacted with $PtCl_2(PhCN)_2$ in refluxing benzene resulting in the easily isolable complexes **1a**, **2a** and **3a**,

respectively (Scheme 2). In dichloromethane one Pt–Cl bond of these $PtCl_2(L)$ complexes inserts tin(II)chloride yielding $PtCl(SnCl_3)(L)$-type products. The solubility of these complexes is unexpectedly low. While $PtCl(SnCl_3)(\mathbf{2})$ and $PtCl(SnCl_3)(\mathbf{3})$ were crystallised slowly from the reaction mixture, $PtCl(SnCl_3)(\mathbf{1})$ proved to be practically insoluble in halogenated solvents and precipitated immediately upon addition of $SnCl_2$.

The ^{31}P-NMR spectra of the $PtCl_2(L)$ complexes show a characteristic pair of doublets corresponding to an AX spin system. Each of these lines is flanked by platinum satellites resulting in a characteristic 1/4/1 pattern with $^1J(^{31}P,^{195}Pt)$ coupling constants of about 3700 and 3500 Hz for **1a**, **3a** and **2a**, respectively, clearly indicating the presence of the chloro ligands trans to phosphorus.

The in situ tin(II)chloride insertion reaction was followed by ^{31}P-NMR and revealed some differences in reactivity and selectivity of the $PtCl_2(L)$ complexes. The dichloro platinum complexes **1a**, **2a** and **3a** were reacted with tin(II)chloride giving the insertion products (the corresponding platinum–trichlorostannato complexes) in 60, 45 and 30% yield.

The selectivity of insertion is completely different for **2a** and **3a**. While in the case of **3a** the tin(II)chloride insertion takes place selectively trans to the phosphorus attached directly to the Cp ring yielding **3b** exclusively,
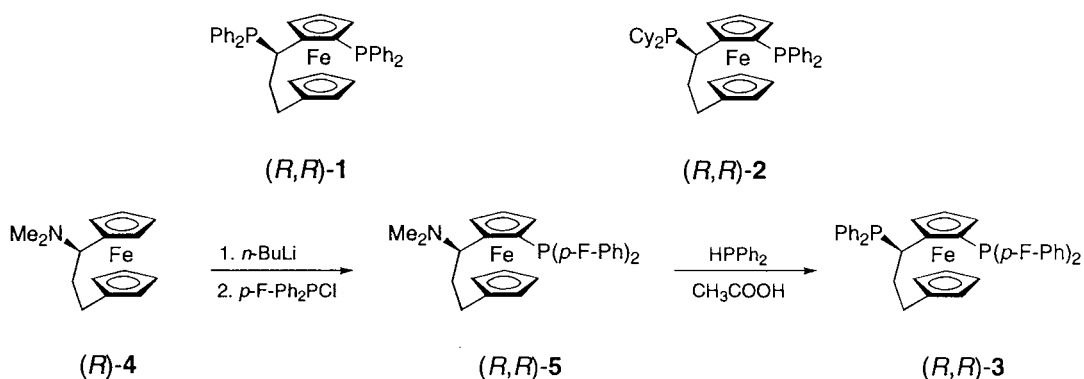
Scheme 1.
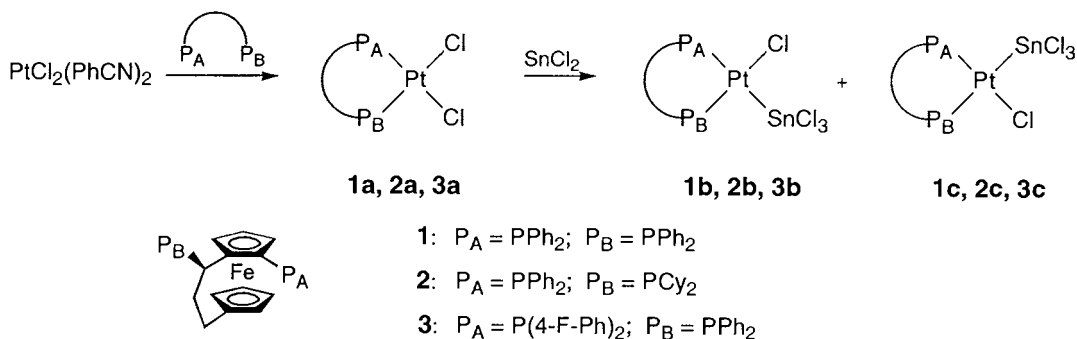
Scheme 2.

Table 1
NMR data of the platinum complexes of ligands 1–3 [a]

	δP_A [b] (ppm)	δP_B [c] (ppm)	$J(^{195}Pt,^{31}P_A)$ (Hz)	$J(^{195}Pt,^{31}P_B)$ (Hz)	$J(P_A-P_B)$ (Hz)	$J(P_A-Sn)$ [d] (Hz)	$J(P_B-Sn)$ (Hz)
1 [e]	−22.3	−6.6	–	–	79.7	–	–
2 [e]	−23.8	9.65	–	–	27.7	–	–
3 [e]	−24.6	−5.87	–	–	83.0	–	–
PtCl$_2$(1) 1a	−2.0	34.4	3375	3715	19.5	–	–
PtCl(SnCl$_3$)(1) 1b	−10.2	27.3	ca. 3300	ca. 3600	24.0	e	e
1c	−9.1	10.2	ca. 2850	ca. 3400	25.6		
PtCl$_2$(2) 2a	−0.4	47.0	3570	3527	16	–	–
PtCl(SnCl$_3$)(2) 2b	8.5	59.4	2931	3426	16	4220, 4408	193
2c	0.2	53.7	3446	2921	15	205	3630, 3812
PtCl$_2$(3) 3a	−4	34	3381	3690	20.2	–	–
PtCl(SnCl$_3$)(3) 3b	−4.8	33	2681	3441	20	e	e

[a] Spectra were measured in CDCl$_3$, 1b and 1c in DMSO-d_6.
[b] P$_A$, PAr$_2$ attached to the Cp ring.
[c] P$_B$, PAr$_2$ or PCy$_2$ attached to the trimethylene bridge.
[d] ^{117}Sn and ^{119}Sn satellites are separately detectable for J_{trans} but coincide for J_{cis}.
[e] Unresolved because of low solubility and/or low resolution.

a 40:60 mixture of 2b and 2c was formed starting from 2a. Since 1b and 1c proved to be completely insoluble in CDCl$_3$ and CD$_2$Cl$_2$, NMR measurements were carried out in DMSO-d_6. Neither 1b nor 1c could be observed in this solvent since the equilibrium (1) lies by far on the left side and only the typical AX spin system of 1a was observed. However, both trichlorostannato complexes 1b and 1c were obtained in about 90% conversion upon addition of a tenfold excess of tin(II)chloride.

$$1a + SnCl_2 \rightleftharpoons 1b + 1c \qquad (1)$$

Only in the case of 2b and 2c could the formation of a direct platinum–tin bond unequivocally be shown by NMR. The presence of both cis and trans tin satellites in the ^{31}P-NMR spectra ($^2J_{cis}(^{117,119}Sn,^{31}P) \approx 200$ Hz and $^2J_{trans}(^{117}Sn,^{31}P) < ^2J_{trans}(^{119}Sn,^{31}P) \approx 4000$ Hz, respectively) is a direct proof of the Pt–SnCl$_3$ moiety (Table 1). In all other cases either the low resolution (3b) or the fast exchange of SnCl$_2$ in DMSO (1b, 1c) made it impossible to determine exactly the $^2J(Sn,P)$ coupling constants. However, the Raman spectrum of PtCl(SnCl$_3$)(1) shows strong bands at 336 and 313 cm^{-1} (and a weak band at 295 cm^{-1}), which can be assigned to the Sn–Cl and Pt–Cl bonds, respectively.

2.3. Structural characterisation of 1a and 2a by X-ray diffraction

The racemic PtCl$_2$ complexes of 1a and 2a were recrystallised from CHCl$_3$–hexane yielding the air-stable orange solvates 1a·CHCl$_3$ and 2a·CHCl$_3$, which were investigated by X-ray diffraction. They crystallise in the centrosymmetric monoclinic space groups $P2_1/n$ and $P2_1/c$, respectively, each with four symmetry equivalent formula units in the unit cell. Crystallographic and experimental data are given in Table 2. Plots of the molecular structures are shown in Figs. 1 and 2. Selected geometric data are presented in Table 3. The general structural features of the ferrocenyl ligands are similar to those of related heteroannularly bridged derivatives [21]. The Cp rings of both complexes adopt approximately eclipsed configurations. The C$_3$ bridges linking the Cp rings force them into a tilted configuration with Cp–Cp tilt angles of 9.8(2)° (1·HCl$_3$) and 10.4(2)° (2a·CHCl$_3$). In addition, the benzylic C atoms are significantly displaced out of the Cp ring planes and toward each other: for 1a·CHCl$_3$ by 0.136(5) Å (C1) and 0.155(6) Å (C3), for 2a·CHCl$_3$ by 0.129(4) Å (C1) and 0.166(5) Å (C3). The atoms coordinated to platinum (2 P and 2 Cl atoms) exhibit the usual distorted square planar arrangement. The mean bond lengths of the PtP$_2$Cl$_2$ squares of the two compounds agree almost perfectly, with bond lengths of 2.240 Å for the Pt–P bonds of both complexes and with 2.356 and 2.357 Å for the Pt–Cl bonds of 1a·CHCl$_3$ and 2a·CHCl$_3$, respectively. Despite the similar appearance of both complexes in the region of the PtP$_2$Cl$_2$ quadrangles (Figs. 1 and 2), a significant difference in the inclination angle of the best plane through PtP$_2$Cl$_2$ and through the Cp (2) ring (C21–C25) does exist, with angles of 27.8(1)° in 1a·CHCl$_3$ and 39.8(1)° in 2a·CHCl$_3$. The difference in

Table 2
Crystallographic data for **1a**·CHCl$_3$ and **2a**·CHCl$_3$

	1a·CHCl$_3$	**2a**·CHCl$_3$
Formula	C$_{38}$H$_{33}$Cl$_5$FeP$_2$Pt	C$_{38}$H$_{45}$Cl$_5$FeP$_2$Pt
fw	979.77	991.87
Crystal size (mm)	0.12 × 0.24 × 0.24	0.10 × 0.14 × 0.32
Space group	$P2_1/n$ (No. 14)	$P2_1/c$ (No. 14)
a (Å)	12.810(4)	13.267(4)
b (Å)	18.040(6)	15.647(5)
c (Å)	16.410(5)	19.576(7)
β (°)	99.54(2)	109.41(2)
V (Å^3)	3740(2)	3833(2)
Z	4	4
T (K)	299(2)	299(2)
D_{calc} (g cm^{-3})	1.740	1.719
$F(000)$	1920	1968
μ(Mo-K$_\alpha$) (mm^{-1})	4.59	4.48
Absorption correction	Multi scan	Multi scan
Transmission fact. Min/max	0.555/0.802	0.557/0.802
θ_{max} (°)	30	30
Index ranges	$-18 \leq h \leq 18$	$-18 \leq h \leq 18$
	$-25 \leq k \leq 25$	$-22 \leq k \leq 21$
	$-23 \leq l \leq 23$	$-27 \leq l \leq 27$
No. of reflections measured	58 884	60 259
No. of unique reflections	10 858	11 137
No. of reflections $I < 2\sigma(I)$	8674	8983
No. of parameters	425	425
R_1 ($I < 2\sigma(I)$)	0.027	0.023
R_1 [a] (all data)	0.043	0.039
wR_2 [b] (all data)	0.062	0.051
Difference Fourier peaks min/max (e Å^{-3})	−1.06/1.01	−0.69/0.64

[a] $R_1 = \Sigma||F_o| - |F_c||/\Sigma|F_o|$.

[b] $wR_2 = [\Sigma(w(F_o^2 - F_c^2)^2)/\Sigma(w(F_o^2)^2)]^{1/2}$.
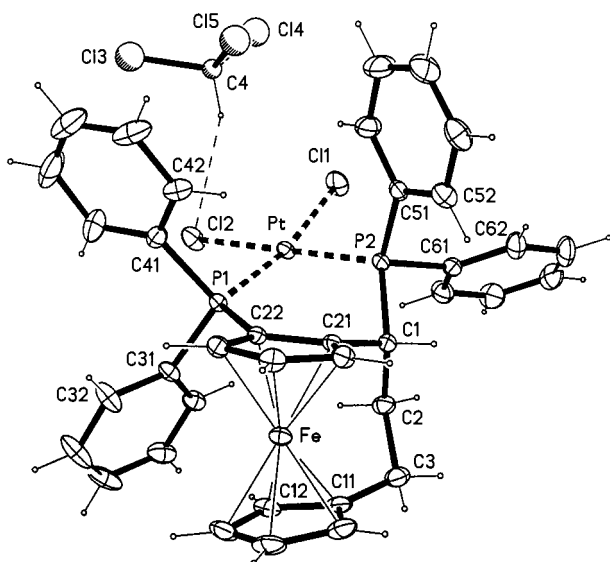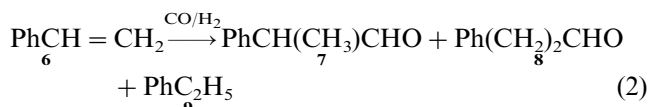

Fig. 1. Structural view of **1a**·CHCl$_3$ showing 20% probability thermal ellipsoids. The CHCl$_3$ solvent molecule and its hydrogen bond to Cl2 (thin dashed line) is included.

these interplanar angles corresponds to positional differences of 0.4 Å for Pt and 0.8 Å for Cl, when the ferrocene moieties, C$_3$ bridges, and P2 atoms of both complexes are fitted so as to coincide. We attribute this variation to crystal packing effects and in particular to remarkable interactions of the CHCl$_3$ solvent molecule with the PtP$_2$Cl$_2$ quadrangle: in **1a**·CHCl$_3$ the CHCl$_3$ is located *above* the PtP$_2$Cl$_2$ quadrangle (Fig. 1) showing a bent hydrogen bond C4–H4···Cl2 (C4···Cl2 = 3.538 Å, H4···Cl2 = 2.62 Å, C4–H4···Cl2 = 156°) and a weak Pt···Cl5 interaction of 4.32 Å; in **2a**·CHCl$_3$ the CHCl$_3$ is located *below* the PtP$_2$Cl$_2$ quadrangle (Fig. 2) showing a bifurcated hydrogen bond C4–H4···Cl1, Cl2 (C4···Cl1 = 3.645 Å, H4···Cl1 = 2.80 Å, C4–H4···Cl1 = 145°, C4···Cl2 = 3.456 Å, H4···Cl2 = 2.63 Å, C4–H4···Cl2 = 142°) and a weak Pt···Cl3 interaction of 4.59 Å. Apart from influencing the specific conformations of both complexes these interactions between CHCl$_3$ and the PtP$_2$Cl$_2$ quadrangles may contribute significantly to the pronounced stability of both compounds against solvent loss (airstable for months). Fig. 3 shows plots of superpositions of the complexes with their free ligands [22]. These plots show that complexation of platinum is accompanied by the following structural changes: (i) by a signficant out-of-plane deformation of the P1 atoms from the Cp rings to which they are attached: −0.041(3) and 0.105(3) Å in the free ligands, 0.330(5) and 0.344(4) Å in the PtCl$_2$ complexes; (ii) by a decrease of the P1–P2 distances from 3.49 and 3.69 Å in the free ligands to 3.313(1) Å in **1a**·CHCl$_3$ and 3.359(1) Å **2a**·CHCl$_3$; and (iii) by a significant rotation of the Cp-bonded diphenylphosphines about the P1–C22 bond axes bringing the phenyl ring 3 (C31–C36) in close proximity to H12, a fact which is also causing a signficant upfield-shift of the NMR signals of this particular proton. The outlined features of the two complexes are consistent with a relatively stiff ligand backbone and little conformational freedom in the region of the PtP$_2$Cl$_2$ quadrangles.

2.4. Homogeneous carbonylation of styrene with platinum and palladium catalysts

2.4.1. Hydroformylations

Styrene (**6**) as the model substrate was reacted in the presence of one of the platinum-containing precursors **1a**, **2a** or **3a** and anhydrous tin(II)chloride with CO–H$_2$ (1:1) at 60–100°C and at a pressure of 100 bar (Table 4).

$$\underset{\mathbf{6}}{PhCH = CH_2} \overset{CO/H_2}{\longrightarrow} \underset{\mathbf{7}}{PhCH(CH_3)CHO} + \underset{\mathbf{8}}{Ph(CH_2)_2CHO}$$
$$+ \underset{\mathbf{9}}{PhC_2H_5} \qquad (2)$$

In each case in addition to the formyl regioisomers **7** and **8** the hydrogenation product **9** was also formed (reaction (2), Table 4).
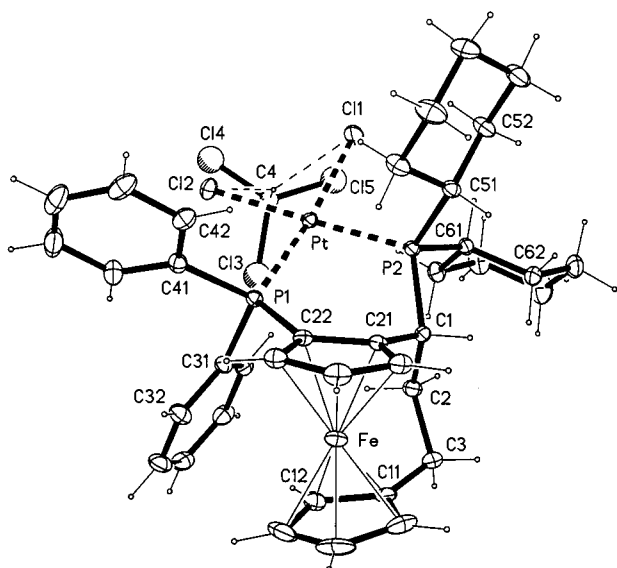
Fig. 2. Structural view of **2a**·CHCl$_3$ showing 20% probability thermal ellipsoids. The CHCl$_3$ solvent molecule behind the PtP$_2$Cl$_2$ quadrangle and its bifurcated hydrogen bond to Cl1 and Cl2 (thin dashed line) is included.

Although the activity of the tested platinum catalysts falls behind that of most of the Pt–diphosphine–tin(II)chloride systems, the ferrocenyl–diphosphine-based catalysts proved to be of interest from a theoretical point of view.

It is worth noting that both the chemoselectivity of hydroformylation and the regioselectivity towards the branched aldehyde are significantly influenced by the basicity of the diphosphine ligands. The use of the most basic ligand **2** results in the lowest chemo- and regioselectivities. Variation of the temperature did not significantly change the regioselectivity. However, when **1a** and **2a** were used as the catalyst precursor a strong temperature dependence of the enantioselectivity was observed. At low temperature the formation of (*R*)-2-phenyl-propanal and at higher temperature (above 70°C) that of the (*S*)-enantiomer is favoured.

Although similar phenomena have previously been observed for other (*C$_2$*-symmetrical) bidentate phosphines [14,16], the temperature dependence of the catalytic systems with ligands **1** and **2** is remarkable. In general, the strong temperature dependence of the enantioselectivity of platinum–diphosphine–tin(II)chloride-catalysed hydroformylations is explained by invoking both kinetic and steric factors. The change in enantiomeric excess of the product might primarily be determined by differences in the temperature dependence of the reaction paths involving the diastereomeric transition states that are formed by coordinating the prochiral substrate with either its *re* or its *si* site to the metal fragment. When the reaction rates related to these diastereomeric pathways show a significantly different temperature

dependence, a change of the predominating enantiomer can occur. A second explanation takes into account the possibility of a ligand flexibility, which in a complex could result in conformer equilibria. A strong temperature dependence of such an equilibrium is likely to influence the face selectivity of a substrate, thus influencing the enantioselectivity and the absolute configuration of the product. In the case of our rigid heteroannularly bridged ferrocenyl ligands, conformer equilibria caused by the ligands can be ex-

Table 3
Selected bond distances (Å) and angles (°) for **1a**·CHCl$_3$ and **2a**·CHCl$_3$

	1a·CHCl$_3$	**2a**·CHCl$_3$
Bond distances		
Pt–P(1)	2.240(1)	2.237(1)
Pt–P(2)	2.240(1)	2.243(1)
Pt–Cl(1)	2.348(1)	2.357(1)
Pt–Cl(2)	2.364(1)	2.356(1)
Fe–C(11)	2.015(3)	2.019(3)
Fe–C(12)	2.040(3)	2.049(3)
Fe–C(13)	2.054(3)	2.071(3)
Fe–C(14)	2.053(3)	2.041(3)
Fe–C(15)	2.026(3)	2.027(3)
Fe–C(21)	2.016(3)	2.017(2)
Fe–C(22)	2.042(3)	2.053(2)
Fe–C(23)	2.049(3)	2.057(3)
Fe–C(24)	2.046(3)	2.041(3)
Fe–C(25)	2.033(3)	2.024(3)
	2.037	2.040
P(1)–C(22)	1.798(3)	1.811(2)
P(1)–C(31)	1.812(3)	1.814(2)
P(1)–C(41)	1.822(3)	1.823(3)
P(2)–C(1)	1.852(3)	1.856(2)
P(2)–C(51)	1.815(3)	1.865(2)
P(2)–C(61)	1.831(3)	1.845(2)
Bond angles		
P(1)–Pt–P(2)	95.37(3)	97.14(3)
P(1)–Pt–Cl(1)	169.09(3)	173.23(2)
P(1)–Pt–Cl(2)	86.51(3)	87.28(3)
P(2)–Pt–Cl(1)	91.16(4)	88.50(3)
P(2)–Pt–Cl(2)	177.88(3)	174.98(2)
Cl(1)–Pt–Cl(2)	87.14(4)	87.25(3)
Pt–P(1)–C(22)	117.1(1)	114.4(1)
Pt–P(1)–C(31)	114.9(1)	113.5(1)
Pt–P(1)–C(41)	106.4(1)	111.2(1)
C(22)–P(1)–C(31)	107.4(1)	108.3(1)
C(22)–P(1)–C(41)	101.9(1)	103.3(1)
C(31)–P(1)–C(41)	107.9(2)	105.2(1)
Pt–P(2)–C(1)	114.6(1)	115.8(1)
Pt–P(2)–C(51)	112.7(1)	112.4(1)
Pt–P(2)–C(61)	113.3(1)	112.8(1)
C(1)–P(2)–C(51)	105.2(1)	103.2(1)
C(1)–P(2)–C(61)	103.6(1)	106.1(1)
C(51)–P(2)–C(61)	106.6(1)	105.6(1)
C(21)–C(1)–C(2)	115.3(2)	114.1(2)
C(1)–C(2)–C(3)	114.3(3)	114.1(2)
C(2)–C(3)–C(11)	114.0(3)	114.5(2)

(a) **(b)**

Fig. 3. Superposition plots of (a) **1a**·CHCl$_3$ and the free ligand **1** (dashed lines), and of (b) **2a**·CHCl$_3$ and the free ligand **2** (dashed lines). Note the significant out-of-plane bending of the Cp-bonded phosphorus in the PtCl$_2$ complexes.

Table 4
Hydroformylations and hydromethoxycarbonylations with use of ligands **1**–**3**

Catalyst	T (°C)	Reaction time (h)	Conversion (%)	R_c [c] (%)	R_{RB} [d] (%)	e.e. (%)
PtCl$_2$(**1**)+SnCl$_2$ [a]	60	40	41	87	46	38 (R)
PtCl$_2$(**1**)+SnCl$_2$	100	35	99	71	50	2 (S)
PtCl$_2$(**2**)+SnCl$_2$	40	120	77	74	32	19 (R)
PtCl$_2$(**2**)+SnCl$_2$	60	20	68	70	34	5 (R)
PtCl$_2$(**2**)+SnCl$_2$	90	20	99	62	37	31 (S)
PtCl$_2$(**2**)+SnCl$_2$	100	16	83	67	36	37 (S)
PtCl$_2$(**3**)+SnCl$_2$	60	100	62	85	45	36 (R)
PdCl$_2$(PhCN)$_2$+**1** [b]	100	160	41	>99	13	n.d.
PdCl$_2$(PhCN)$_2$+**2**	100	160	70	>99	14	n.d.

[a] Hydroformylations: $p = 100$ bar CO/H$_2 = 1/1$.
[b] Hydromethoxycarbonylations: $p = 100$ bar CO.
[c] Chemoselectivity towards hydroformylation.
[d] Regioselectivity towards branched aldehyde.

cluded and hence the former explanation for the change in the absolute configuration of the product seems to be more appropriate.

2.4.2. Hydromethoxycarbonylations

Catalyst precursors prepared in situ from PdCl$_2$(PhCN)$_2$ and either of the enantiopure ferrocenyl ligands **1**, **2** or **3** have been tested in the hydromethoxy-carbonylation of styrene (Eq. (3)). The catalytic activity of these systems was found to be unexpectedly low. Acceptable conversion was only obtained after a prolonged reaction time of about 1 week.

$$\text{PhCH} = \text{CH}_2 \xrightarrow{\text{CO/CH}_3\text{OH}} \text{PhCH(CH}_3)\text{COOCH}_3$$
$$\mathbf{6} \qquad\qquad\qquad \mathbf{10}$$
$$+ \text{Ph(CH}_2)_2\text{COOCH}_3 \qquad (3)$$
$$\mathbf{11}$$

In all cases both regioisomers were formed but with the linear ester (**11**) being the main product.

3. Experimental

3.1. General procedures

All reactions were carried out under argon using standard Schlenk techniques. Toluene was distilled from sodium in the presence of benzophenone. Diethyl ether and benzene were distilled from LiAlH$_4$. Styrene was freshly distilled before use.

NMR spectra were recorded in CDCl$_3$ (if not otherwise noted) on either a Bruker AM 400 WB spectrometer at 400.13 MHz (^{1}H), 100.62 MHz (^{13}C) and 161.89 MHz (^{31}P), or on a Varian Unity at 300 spectrometer 121.4 MHz (^{31}P), respectively. Chemical shifts δ are reported in ppm relative to CHCl$_3$ (7.26 and 77.00 ppm for ^{1}H and ^{13}C) or relative to H$_3$PO$_4$ (^{31}P). The coupling constants in ^{13}C-NMR spectra refer to J_{CP} unless otherwise stated. Mass spectra were measured on a

Finnigan 900S spectrometer (E.I., 70eV). Optical rotations were measured on a Perkin–Elmer polarimeter 241 in chloroform at 20°C. Elemental analyses were either performed at Mikroanalytisches Laboratorium der Universität Wien (Mag. J. Theiner) or were measured on a 1108 Carlo Erba apparatus.

The catalytic precursors $PtCl_2(PhCN)_2$ and $PdCl_2$-$(PhCN)_2$ were prepared as described previously [23,24]. Samples of the catalytic reactions were analysed with a Hewlett–Packard 5830A gas chromatograph fitted with a capillary column coated with OV-1.

3.2. Synthesis of (R,R)-1-[bis-(4-fluorophenyl)-phosphino-2,1′-(1-dimethylamino)-propanediyl] ferrocene (5)

To a degassed solution of 1 g (3.72 mmol) of (S)-1,1′-[(1-dimethylamino)-propanediyl] ferrocene, 4, in 20 ml of ether was added dropwise 2.8 ml (4.48 mmol) of a 1.6 M solution of butyllithium in hexane at 0°C. The reaction mixture was stirred at room temperature (r.t.) for 4 h and then 0.8 ml (4.56 mmol) of chloro-bis-(4-fluorophenyl)-phosphine was added at r.t. After stirring for 16 h the mixture was hydrolysed with 30 ml of aqueous sodium hydrogencarbonate. The organic and the aqueous layers were separated and the aqueous layer was extracted twice with 25 ml portions of ether. The combined organic layers were washed with water and dried over magnesium sulfate. After removing the solvent under reduced pressure the product was purified by chromatography on silica gel. Petroleum ether as the eluent removes unpolar inpurities while a 20:80 mixture of methanol and chloroform elutes 1.33 g (2.72 mmol, 73%) of the enantiomerically pure product.

^{1}H-NMR: δ 1.81 (s, 6H), 1.83–1.91 (m, 1H), 2.37–2.46 (m, 2H), 2.57–2.63 (m, 1H), 2.90–2.95 (m, 1H), 3.63 (m, 1H, Cp), 3.70 (m, 1H, Cp), 3.86 (m, 1H, Cp), 4.08 (m, 1H, Cp), 4.14 (m, H, Cp), 4.18 (m, 1H, Cp), 4.31 (m, 1H, Cp), 6.91–7.02 (m, 4H, Ph), 7.26–7.32 (m, 2H, Ph), 7.36–7.41 (m, 2H, Ph). ^{13}C-NMR: δ 25.47 (CH$_2$), 38.27 (d, $J = 9.9$ Hz, CH$_2$), 44.24 (CH$_3$), 66.44 (d, $J = 1.5$ Hz, CH), 67.75 (CH), 69.31 (CH), 70.13 (CH), 71.42 (d, $J = 6.1$ Hz, CH), 71.58 (CH), 73.55 (d, $J = 4.6$ Hz, CH), 74.39 (d, $J = 4.6$ Hz, CH), 75.53 (d, $J = 12.2$ Hz, q-C), 88.68 (q-C), 114.74 (dd, $J = 6.9$ Hz, $J_{CF} = 13.0$ Hz, Ph), 114.95 (dd, $J = 6.9$ Hz, $J_{CF} = 13.0$ Hz, Ph), 134.15 (d, $J = 13.0$ Hz, q-Ph), 134.89 (dd, $J = 8.4$ Hz, $J_{CF} = 3.1$ Hz, q-Ph), 135.15 (dd, $J = 21.4$ Hz, $J_{CF} = 7.7$ Hz, Ph), 135.76 (dd, $J = 21.4$ Hz, $J_{CF} = 8.4$ Hz, Ph), 162.84 (d, $J_{CF} = 247.0$ Hz, q-Ph), 163.00 (d, $J_{CF} = 248.6$ Hz, q-Ph). ^{31}P-NMR: δ −23.02 (dd, $J_{1,PF} = J_{2,PF} = 4.0$ Hz).

MS: m/e (rel. %) 489.0 (33.4, M$^+$), 474.0 (24.0), 446.0 (30.9), 294.1 (32.4), 264.9 (30.8), 251.0 (100), 237.0 (59.4), 211.1 (25.6), 149.0 (32.4).

$[\alpha]^{20}$ (°, λ) + 177.5 (589), + 177.2 (578), + 156.4° (546); $c = 0.994$.

Anal. Calc. for C$_{27}$H$_{26}$F$_2$FeNP ($M = 489.11$): C, 66.26; H, 5.32; N, 2.86; P, 6.34. Found: C, 65.99; H, 5.19; N, 2.77; P, 6.60%.

3.3. Synthesis of (R,R)-1-bis(4-fluorophenyl)-phosphino-2,1′-[(1-diphenylphosphino)-1,3-propanediyl]-ferrocene (3)

To a degassed solution of 700 mg (1.43 mmol) of (+)-aminophosphine 5 in 13 ml of freshly distilled acetic acid was added 0.4 ml (2.3 mmol) of diphenylphosphine. The solution was stirred for 18 h at 90°C. After cooling to r.t., the product crystallises and is filtered off, washed with petroleum ether and dried in vacuo giving 622 mg (0.99 mmol, 69%) of 3.

^{1}H-NMR: δ 1.60–1.68 (m, 1H), 2.09–2.15 (m, 1H), 2.47–2.52 (m, 1H), 2.76–2.80 (m, 1H), 2.96–2.99 (m, 1H), 3.54 (s, 1H, Cp), 3.68 (s, 1H, Cp), 3.87 (s, 1H, Cp), 4.11 (s, 1H, Cp), 4.16 (s, 1H, Cp), 4.27 (s, 1H, Cp), 4.31 (s, 1H, Cp), 6.78–6.83 (m, 2H, Ph), 7.03–7.06 (m, 4H, Ph), 7.11–7.21 (m, 5H, Ph), 7.27–7.33 (m, 3H, Ph), 7.41–7.46 (m, 2H, Ph), 7.51–7.56 (m, 2H, Ph). ^{13}C-NMR: δ 25.15 (d, $J = 10.7$ Hz, CH$_2$), 37.23 (dd, $J_1 = 3.1$ Hz, $J_2 = 13.8$ Hz, CH), 38.49 (dd, $J_1 = 10.0$ Hz, $J_2 = 25.2$ Hz, CH$_2$), 67.92 (Cp), 69.77 (Cp), 69.95 (Cp), 71.12 (d, $J = 4.6$ Hz, Cp), 71.82 (Cp), 73.86 (d, $J = 3.8$ Hz, Cp), 74.07 (d, $J = 14.5$ Hz, q-Cp), 76.38 (dd, $J_1 = 2.3$ Hz, $J_2 = 4.6$ Hz, Cp), 87.40 (q-Cp), 90.94 (dd, $J_1 = 16.8$ Hz, $J_2 = 21.4$ Hz, q-Cp), 114.88 (dd, $J = 6.9$ Hz, $J_{CF} = 13.0$ Hz, Ph), 114.98 (dd, $J = 7.7$ Hz, $J_{CF} = 12.2$ Hz, Ph), 127.66 (d, $J = 6.9$ Hz, Ph), 128.27 (d, $J = 7.7$ Hz, Ph), 128.31 (Ph), 128.78 (Ph), 133.45 (d, $J = 19.9$ Hz, Ph), 133.49 (d, $J = 20.7$ Hz, Ph), 133.98 (q-Ph), 134.66 (dd, $J = 19.1$ Hz, $J_{CF} = 7.7$ Hz, Ph), 135.70 (q-Ph), 136.56 (dd, $J = 22.2$ Hz, $J_{CF} = 7.7$ Hz, Ph), 137.09 (d, $J = 16.1$ Hz, q-Ph), 139.73 (dd, $J = 20.7$ Hz, $J_{CF} = 3.8$ Hz, q-Ph), 162.65 (d, $J_{CF} = 247.1$ Hz, q-Ph), 163.23 (d, $J_{CF} = 249.4$ Hz, q-Ph). ^{31}P-NMR: δ − 5.34 (d, $J_{PP} = 82.3$ Hz); − 24,09 (ddd, $J_{1(PF)} = 4.2$ Hz, $J_{2(PF)} = 4.4$ Hz, $J_{PP} = 82.3$ Hz). MS: m/z (rel. %): 630.4 (46.6, M$^+$), 445.0 (100), 223.9 (44.5).

$[\alpha]^{20}$ (°, λ) + 165.5 (589), + 167.5 (578), + 162.7 (546); $c = 1.024$.

Anal. Calc. for C$_{37}$H$_{30}$F$_2$FeP$_2$ ($M = 630.11$): C, 70.48; H, 4.76; P, 9.84. Found: C, 69.74; H, 4.78; P, 9.95%.

3.4. Synthesis of PtCl$_2$(1), (1a), PtCl$_2$(2), (2a) and PtCl$_2$(3), (3a)

A degassed solution of 46.7 mg (0.099 mmol) of dibenzonitrilo platinum(II)chloride in 6 ml of benzene was heated to 80–90°C for about 5 min. To this solution was added a degassed solution of 0.1 mmol diphosphine. The reaction mixture was refluxed for 1 h

and then stirred at r.t. for another 16 h. The precipitated product was washed with benzene and hexane and dried in vacuum. Yields were in the range of 80–90% for all three complexes.

3.4.1. Compound 1a

Yield: 88%; ^{1}H-NMR: δ 1.54–1.57 (m, 1H), 2.19 (s, 1H, Cp), 2.26–2.35 (m, 2H), 2.52–2.56 (m, 1H), 2.77–2.85 (m, 1H), 3.52 (m, 1H, Cp), 3.78 (m, 1H, Cp), 3.96 (m, 1H, Cp), 4.04 (m, 1H, Cp), 4.11 (m, 1H, Cp), 4.41 (m, 1H, Cp), 6.79–6.85 (m, 2H, Ph), 7.02–7.07 (m, 2H, Ph), 7.18–7.24 (m, 1H, Ph), 7.34–7.43 (m, 5H, Ph), 7.48–7.50 (m, 1H, Ph), 7.54–7.57 (m, 3H, Ph), 7.73–7.78 (m, 2H, Ph), 8.10–8.15 (m, 2H, Ph), 8.27 (bs, 2H, Ph). ^{13}C-NMR: δ 23.78 (d, $J = 13.8$ Hz, CH$_2$), 32.51 (d, $J = 37.5$ Hz, CH), 41.01 (d, $J = 10.7$ Hz, CH$_2$), 69.05 (Cp), 69.09 (d, $J = 7.7$ Hz, Cp), 71.78 (Cp), 72.02 (Cp), 72.35 (Cp), 72.61 (dd, $J_1 = 3.8$ Hz, $J_2 = 8.4$ Hz, Cp), 75.63 (d, $J = 5.4$ Hz, Cp), 87.06 (q-Cp), 89.98 (d, $J = 15.3$ Hz, q-Cp), 126.75 (d, $J = 61.2$ Hz, q-Ph), 127.39 (d, $J = 11.5$ Hz, Ph), 127.66 (d, $J = 11.5$ Hz, Ph), 127.83 (d, $J = 12.2$ Hz, Ph), 128.54 (d, $J = 10.7$ Hz, Ph), 129.44 (d, $J = 60.4$ Hz, q-Ph), 129.97 (d, $J = 3.1$ Hz, Ph), 131.09 (d, $J = 3.1$ Hz), 131.13 (d, $J = 71.9$ Hz, q-Ph), 131.59 (d, $J = 3.1$ Hz, Ph), 131.69 (d, $J = 3.1$ Hz, Ph), 133.10 (d, $J = 10.0$ Hz, Ph), 33.39 (d, $J = 68.8$ Hz, q-Ph), 134.25 (d, $J = 10.6$ Hz, Ph), 135.25 (d, $J = 10.7$ Hz, Ph), 136.41 (d, $J = 10.7$ Hz, Ph). ^{31}P-NMR: see Table 1.

$[\alpha]^{20}$ (°, λ) $+9.6$ (589), $+3.3$ (578), -44.3 (546); $c = 0.519$.

Anal. Calc. for C$_{37}$H$_{32}$Cl$_2$FeP$_2$Pt ($M = 860.44$): C, 51.65; H, 3.75. Found: C, 51.94; H, 4.02%.

3.4.2. Compound 2a

Yield: 84%. ^{1}H-NMR: δ 0.95–1.81 (m, 18H), 1.85 (s, 1H, Cp), 1.85–1.92 (m, 2H), 1.99–2.05 (m, 1H), 2.11–2.13 (m, 1H), 2.23–2.28 (m, 1H), 2.37 (m, 1H), 2.47–2.51 (m, 1H), 2.59–2.61 (m, 1H), 2.69–2.78 (m, 1H), 3.63 (s, 1H, Cp), 3.76 (s, 1H, Cp), 3.88 (s, 1H, Cp), 4.15 (s, 2H, Cp), 4.32 (s, 1H, Cp), 7.13–7.15 (m, 3H, Ph), 7.17–7.26 (m, 2H, Ph), 7.40–7.44 (m, 3H, Ph), 8.06–8.13 (m, 2H, Ph).

^{13}C-NMR: δ 23.87 (d, $J = 11.5$ Hz, CH$_2$), 25.85 (CH$_2$), 26.36 (CH$_2$), 27.07 (d, $J = 13.0$ Hz, CH$_2$), 27.20 (d, $J = 11.5$ Hz, CH$_2$), 27.58 (d, $J = 11.5$ Hz, CH$_2$), 27.79 (d, $J = 13.0$ Hz, CH$_2$), 28.59 (dd, $J_1 = 2.3$ Hz, $J_2 = 29.8$ Hz, CH), 29.75 (d, $J = 3.8$ Hz, CH$_2$), 30.07 (d, $J = 2.3$ Hz, CH$_2$), 31.01 (CH$_2$), 31.41 (CH$_2$), 36.19 (d, $J = 30.6$ Hz, CH), 38.58 (d, $J = 1.4$ Hz, CH), 40.69 (d, $J = 5.4$ Hz, CH$_2$), 68.76 (d, $J = 8.4$ Hz, Cp), 68.90 (dd, $J_1 = 2.3$ Hz, $J_2 = 63.5$ Hz, q-C), 69.03 (Cp), 71.27 (Cp), 71.87 (Cp), 72.39 (dd, $J_1 = 3.8$ Hz, $J_2 = 7.7$ Hz, Cp), 73.17 (Cp), 76.48 (d, $J = 5.4$ Hz, Cp) 85.90 (q-Cp), 90.68 (d, $J = 18.4$ Hz, q-Cp), 127.33 (d, $J = 18.4$ Hz, Ph), 127.66 (d, $J = 11.5$ Hz, Ph), 130.09 (d, $J = 2.3$ Hz,

Ph), 131.43 (d, $J = 3.1$ Hz, Ph), 131.62 (d, $J = 70.4$ Hz, q-Ph), 133.09 (d, $J = 71.9$ Hz, q-Ph), 133.66 (d, $J = 9.2$ Hz, Ph), 136.66 (bs, Ph). ^{31}P-NMR: see Table 1.

$[\alpha]^{20}$ (°, λ) $+35.8$ (589), $+25.3$ (578), -43.5 (546); $c = 0.495$.

Anal. Calc. for C$_{37}$H$_{44}$Cl$_2$FeP$_2$Pt ($M = 872.55$): C, 50.93; H, 5.08. Found: C, 51.11; H, 5.33%.

3.4.3. Compound 3a

Yield: 83%. ^{1}H-NMR: δ 1.53–1.61 (m, 1H), 2.23–2.29 (m, 1H), 2.34 (s, 1H, Cp), 2.34–2.39 (m, 1H), 2.54–2.57 (m, 1H), 2.77–2.85 (m, 1H), 3.55 (m, 1H, Cp), 3.83 (m, 1H, Cp), 4.00 (m, 1H, Cp), 4.02 (m, 1H, Cp), 4.15 (m, 1H, Cp), 4.44 (m, 1H, Cp), 6.74–6.78 (m, 4H, Ph), 7.24–7.29 (m, 2H, Ph), 7.34–7.45 (m, 5H, Ph), 7.47–7.51 (m, 1H, Ph), 7.70–7.75 (m, 2H, Ph), 8.07–8.12 (m, 2H, Ph), 8.27 (bs, 2H, Ph). ^{31}P-NMR (CDCl$_3$, 161.9 MHz, H$_3$PO$_4$): see Table 1.

Anal. Calc. for C$_{37}$H$_{30}$Cl$_2$F$_2$FeP$_2$Pt ($M = 896.42$): C, 49.58; H, 3.37. Found: C, 49.75; H, 3.52%.

3.5. Hydroformylation experiments with 1a, 2a and 3a

In a typical experiment a solution of 0.025 mmol of PtCl$_2$(2) and 0.05 mmol of SnCl$_2$ in 30 ml of toluene containing 0.1 mol of styrene was transferred under argon into a 150 ml stainless steel autoclave. The reaction vessel was pressurised to 80 bar total pressure (1:1 CO–H$_2$) and the magnetically stirred mixture was heated in an oil bath. The pressure was monitored throughout the reaction. After cooling and venting of the autoclave, the pale yellow solution was immediately analysed by GC, then fractionally distilled. Finally, the specific rotation of the 2-phenylpropanal fraction was determined.

3.6. Hydromethoxycarbonylation experiments

In a typical experiment a 150 ml stainless steel autoclave was charged under argon with 0.04 mmol of PdCl$_2$(PhCN)$_2$, 0.02 mmol of 2, with 1.8 ml of styrene, 10 ml of toluene and 5 ml of methanol. The reaction vessel was pressurised with CO to 130 bar and the magnetically stirred mixture was heated in an oil bath. The pressure was monitored throughout the reaction. After cooling and venting of the autoclave, the dark red solution was immediately analysed by GC.

3.7. X-ray structure determinations of 1a·CHCl$_3$ and 2a·CHCl$_3$

Crystal data and experimental details are given in Table 2. X-ray data for 1a·CHCl$_3$ and 2a·CHCl$_3$ were collected on a Siemens Smart CCD area detector dif-

fractometer (graphite monochromated Mo$-$K$_\alpha$ radiation, $\lambda = 0.71073$ Å, a nominal crystal-to-detector distance of 44.5 mm, 4×606 0.3°-ω-scan frames covering the complete reciprocal space up to $\theta_{max} = 30°$). Corrections for Lorentz and polarization effects, for crystal decay, and for absorption were applied. All structures were solved by direct methods using the program SHELXS-97 [25]. Structure refinement on F^2 was carried out with program SHELXL-97 [26]. Non-hydrogen atoms were refined anisotropically. Hydrogen atoms were inserted in idealized positions and were refined riding with the atoms to which they were bonded.

4. Supplementary material

Crystallographic data (excluding structure factors) for the structure reported in this paper have been deposited with the Cambridge Crystallographic Data Centre, CCDC nos. 118736, 118737. Copies of this information may be obtained free of charge from The Director, CCDC, 12 Union Road, Cambridge, CB2 1EZ, UK (Fax: $+44$-1223-336033; e-mail: deposit@ccdc.cam.ac.uk or www: http://www.ccdc.cam.ac.uk).

Acknowledgements

References

[1] H.M. Colquhoun, D.J. Thompson, M.V. Twigg, Carbonylation. Direct Synthesis of Carbonyl Compounds, Plenum Press, New York, 1991.

[2] B. Cornils, in: J. Falbe (Ed.), New Synthesis with Carbon Monoxide, Springer Verlag, Berlin, 1980, p. 133.

[3] M. Beller, B. Cornils, C.D. Frohning, C.W. Kohlpaintner, J. Mol. Catal. A 104 (1995) 17.

[4] C.D. Frohning, C.W. Kohlpainter, in: B. Cornils, W.A. Herrmann (Eds.), Applied Homogeneous Catalysis with Organometallic Compounds, vol. 1, VCH, Weinheim, 1996, p. 29.

[5] C. Botteghi, S. Paganelli, A. Schionato, M. Marchetti, Chirality 3 (1991) 355.

[6] C. Botteghi, M. Marchetti, S. Paganelli, in: M. Beller, C. Bolm (Eds.), Transition Metals for Organic Synthesis, vol. 2, Wiley–VCH, Weinheim, 1998, p. 25.

[7] H. Brunner, W. Zettlmeier, Handbook of Enantioselective Catalysis with Transition Metal Compounds, VCH, Weinheim, 1993.

[8] S. Gladiali, J.C. Bayón, C. Claver, Tetrahedron: Asymmetry 6 (1996) 1453.

[9] F. Agbossou, J-F. Carpentier, A. Mortreux, Chem. Rev. 95 (1995) 2485.

[10] G. Consiglio, P. Pino, L.I. Flowers, C.U. Pittmann Jr., J. Chem. Soc. Chem. Commun. (1983) 612.

[11] P. Haelg, G. Consiglio, P. Pino, J. Organomet. Chem. 296 (1985) 281.

[12] G. Consiglio, F. Morandini, M. Scalone, P. Pino, J. Organomet. Chem. 279 (1985) 193.

[13] L. Kollár, G. Consiglio, P. Pino, J. Organomet. Chem. 330 (1987) 305.

[14] L. Kollár, J. Bakos, I. Tóth, B. Heil, J. Organomet. Chem. 370 (1989) 257.

[15] G. Consiglio, S.C.A. Nefkens, A. Borer, Organometallics 10 (1991) 2046.

[16] I. Tóth, I. Guo, B. Hanson, Organometallics 12 (1993) 848.

[17] G. Parrinello, J.K. Stille, J. Am. Chem. Soc. 109 (1987) 7122.

[18] A. Togni, T. Hayashi (Eds.), Ferrocenes, VCH, Weinheim, 1995.

[19] B. Jedlicka, W. Weissensteiner, T. Kégl, L. Kollár, J. Organomet. Chem. 563 (1998) 37.

[20] S. Bronco, G. Consiglio, S. Di Benedetto, M. Fehr, F. Spindler, A. Togni, Helv. Chim. Acta 78 (1995) 883.

[21] A. Mernyi, C. Kratky, W. Weissensteiner, M. Widhalm, J. Organomet. Chem. 508 (1996) 209.

[22] T. Sturm, Ph.D. Thesis, University of Vienna, Austria, 1999.

[23] F.R. Hartley, Organomet. Chem. Rev. A 6 (1970) 119.

[24] E.W. Abel, M.A. Bennett, G. Wilkinson, J. Chem. Soc. (1959) 3178.

[25] G.M. Sheldrick, SHELXS-97, Program for the Solution of Crystal Structures, University of Göttingen, Germany, 1997.

[26] G.M. Sheldrick, SHELXL-97, Program for Crystal Structure Refinement, University of Göttingen, Germany, 1997.